Soft Matter

Cite this: *Soft Matter*, 2011, **7**, 8384

www.rsc.org/softmatter

PAPER

Tuning size and electrostatics in non-polar colloidal asphaltene suspensions by polymeric adsorption

Sara M. Hashmi and Abbas Firoozabadi*

Received 5th March 2011, Accepted 30th May 2011
DOI: 10.1039/c1sm05384a

The destabilization of asphaltenes adversely affects many aspects of the petroleum energy industry. Although polymeric dispersants have been shown to stabilize asphaltene colloids in non-polar media, the mechanism by which they prevent aggregation is not well-understood. We use a variety of techniques to investigate systems of colloidal asphaltenes stabilized in heptane by an effective dispersant. Phase analysis light scattering (PALS) measurements reveal an increase in the electrophoretic mobility as a function of dispersant concentration, suggesting electrostatic repulsion as the primary stabilizing force. Dynamic light scattering (DLS) measurements indicate that the increase in mobility corresponds to a decrease in particle size. A simple scaling argument suggests that the dispersant adsorbs to the surface of the asphaltene colloids. UV-visible spectroscopy and static light scattering (SLS) measurements corroborate this proposal. Interestingly, the colloidal asphaltene properties change below the critical micelle concentration (cmc) of the dispersants used. The nature of the asphaltenes themselves plays an important role in allowing for this tunability of their properties. Contrary to currently accepted views of non-polar colloidal suspensions, our results indicate that isolated dispersant molecules, not inverse micelles, can lead to charge-stabilization of asphaltene colloids.

Introduction

Asphaltene precipitation causes significant problems for many aspects of the petroleum energy recovery industry and a multitude of resources have been dedicated to understanding, controlling and inhibiting the precipitation process. Still, questions remain about the mechanisms which take asphaltenes from a molecular-scale dissolved substance to a distinct, separated phase blocking flow, coating equipment or settling during processing. Precipitation can occur with changes in temperature, pressure, or composition. Asphaltene molecules are composed of polyaromatic hydrocarbon ring systems, operationally defined as the oil portion soluble in aromatic liquids but insoluble in light alkanes.[1] Asphaltene molecules associate even in favorable conditions, mainly through π-bonding interactions.[2,3] In unfavorable compositions, asphaltenes aggregate from the scale of tens of nanometres to tens of microns.[4–6] Precipitation proceeds through a state where the asphaltene phase is contained in nano- or micro-scale particles, in the form of colloidal suspensions. Sedimentation follows, with signatures of gelation as observed through light scattering, leading to complete phase separation.[7–9] Bulk solvents can prevent asphaltene precipitation, but their use is neither environmentally friendly nor economically feasible: small doses of effective material to stabilize asphaltenes in suspension at the nano-scale are greatly preferred. A variety of amphiphilic dispersants can preferentially adsorb onto asphaltenes, thereby imparting some stability to the system.[10–15] There have been suggestions that steric stabilization plays a role.[10–12,16] However, measurements that act as proxies for dispersant effectiveness often neglect the dynamics of the precipitation process, and a detailed understanding of dispersant mechanisms remains an open question.[11] At the same time, electrodeposition reveals that asphaltenes are charged entities.[17–19] Asphaltene colloids can be stable even in aqueous and alcohol solutions, with surface charge being tunable by pH and the addition of salts.[20–23] We seek to demonstrate the possibility that electrostatics can stabilize asphaltene colloids in alkanes.

It is energetically unfavorable to separate ions in low dielectric liquids, including alkanes, and therefore electrostatic stabilization in non-polar colloidal suspensions may seem improbable. While the surface grafting of polymers can electrostatically stabilize colloids in aqueous media, their use in non-polar suspensions seems to be limited to providing steric stabilization.[24–26] Notably, non-polar suspensions of polymethyl methacrylate (PMMA) colloids with polyhydroxy stearic acid (PHSA) surface grafts are widely used as model hard sphere systems to investigate the statistical mechanics of fluids and solids.[27–31] While some charge may exist in these sterically-stabilized non-polar colloidal suspensions, it is considered too small to affect the overall system stability.[32,33] However, electrostatic stabilization of carbon black particles was found with the addition of charge control agents, dating back to the pioneering work of van der Minne and Hermanie in the 1950s.[34] The charging mechanism

New Haven, CT, USA. E-mail: abbas.firoozabadi@yale.edu; Fax: +1 203-432-4387; Tel: +1 203-432-4379

was initially postulated to be due to acid–base interactions.[35–37] Subsequent studies using a variety of additives have shown that the electrostatic stabilization can be achieved through inverse micelles.[33,38,39] Pairwise interactions can result in ionic exchange between micelles, or between micelle and colloid. A fraction of micelles can become transiently charged in this manner, facilitating electrostatic interactions between colloids.[40] For instance, when the anionic surfactant dioctyl sodium sulfosuccinate (AOT) is added in excess of its critical micelle concentration (cmc) in dodecane, electrophoretic mobility measurements reveal the generation of colloidal surface charges.[39,41] Despite this detailed understanding of charging in non-polar colloidal suspensions, it is unclear whether dispersant micellization plays a role in colloidal asphaltene stabilization.

Here, we form colloidal asphaltene suspensions in heptane and investigate stabilization by dispersants known to inhibit asphaltene aggregation and sedimentation.[8,9] We show that these dispersants both increase electrophoretic mobility and decrease the size of asphaltene particles by surface adsorption. Remarkably, these changes occur at concentrations below the dispersant cmc. Furthermore, a comparison with AOT suggests that inverse micelles do not necessarily provide the most effective stabilization of asphaltene colloids. The native state of the asphaltenes themselves plays an important role; effective dispersants can halt the continuous growth of asphaltenes to the micron scale. Given our results, we suggest a new mechanism for electrostatic stabilization unique to non-polar colloidal suspensions of asphaltenes.

Materials & methods

Materials

We obtain a petroleum fluid from the Middle East, SB. We precipitate asphaltenes by adding heptane, and define the heptane ratio χ, with units mL g^{-1}, indicating the number of mL heptane (Fischer) mixed with 1 g oil. The asphaltene content of SB is measured as reported previously, by mixing the oil with heptane at $\chi = 40$ mL g^{-1}.[8] The mixtures are soniccated for 1 min, allowed to equilibrate for several hours and filtered through 0.2 μm pore-size cellulose nitrate membrane filters (Whatman). The filtrate is collected, dried and weighed to give the asphaltene weight fraction $f = 0.0069 \pm 0.0008$ g/g. We use a densitometer (Anton Paar) to measure the asphaltene density ρ_a in a solution of 0.005 g asphaltenes in 1 g toluene. Based on 12 measurements, the SB asphaltene density is $\rho_a = 1.1 \pm 0.09$ g mL^{-1}, within error bars of typical literature values.[9]

We obtain proprietary non-ionic dispersants: 0519947BA, which we call BA, a polyolefin alkeneamine with molecular weight ~2000 Da, and 05171004F, which we call 4F, an alkylated phenol with molecular weight ~4000 Da. We use these dispersants as received from Lubrizol Corporation. We obtain dioctyl sodium sulfosuccinate (AOT), with molecular weight 445 Da (Sigma Aldrich). We prepare dispersant stock solutions in heptane at various concentrations c, in ppm by weight. We measure c_c, the critical micelle concentration, of the dispersants in heptane by monitoring the normalized intensity of scattered light I/I_0 at a wave vector $q = 0.02320$ nm^{-1}. We corroborate c_c through conductivity measurements on the dispersants in heptane (Scientifica 600).

Light scattering

A model oil asphaltene solution is prepared by dissolving asphaltenes in toluene at an asphaltene concentration $f_a = 5000$ ppm by weight. All colloidal asphaltene suspensions are made by mixing the model oil with heptane at $\chi = 20$ mL g^{-1}. We mix heptane with dispersant stock solutions at various ratios to obtain normalized concentrations between $0.01 < c/c_c < 100$. Asphaltene suspensions are prepared at volumes of 3 mL and sonicated for 1 min before measurement. The amount of asphaltenes in each suspension is ~340 ppm, corresponding to a colloidal volume fraction $\phi \sim 2.3 \times 10^{-4}$. We assess the effects of dispersant by measuring the electrophoretic mobility μ of the asphaltene colloids using phase-analysis light scattering (ZetaPALS, Brookhaven Instruments). Ten measurements are taken per sample; between 2 and 10 samples are measured at each dispersant concentration assessed: compositions with a larger spread in results require a larger number of samples. To characterize colloidal size and morphology, we use dynamic light scattering at wave vector $q = 0.01872$ nm^{-1} and static light scattering over a range $0.00484 < q < 0.03184$ nm^{-1}. DLS measurements are taken every 30 s for at least 60 min, and are performed on 3–4 samples at each dispersant concentration (ZetaPALS). Scattered light intensity monitoring confirms the absence of sedimentation during this time. SLS measurements are taken every 1°, with a 20 s collection time (ALV-GmbH).

UV-visible spectroscopy

UV-visible spectroscopy is performed on 3 systems: asphaltene solutions in toluene, dispersants in heptane, and colloidal asphaltene suspension supernatants (Agilent 8453). All measurements are done in quartz cuvettes (Cole Parmer), transparent into the UV range. Stock solutions of dispersants in heptane and asphaltene solutions in toluene are used to calibrate the extinction coefficient ε for each material: $A = \varepsilon c L$, where A is the absorbance, c the concentration and $L = 10$ mm, the optical path length for all samples. The asphaltene spectral signature falls within the UV range and extends into the visible range. At low concentrations of asphaltenes in toluene, A is linear with concentration at wavelengths above $\lambda \sim 280$ nm, but saturates at lower wavelengths. We use $\lambda = 575$ nm to characterize the asphaltene concentration, a wavelength at which the dispersants have no residual signatures. At $\lambda = 575$ nm, A is constant with c below $c \sim 140$ ppm. Using several known concentrations of asphaltenes in toluene, we measure $\varepsilon = 0.0191$ (1/ppm 1/mm). The spectra of the dispersants in heptane have signatures in the UV and near UV ranges. Using the dispersant solutions in heptane, we measure $\varepsilon_{BA} = 0.0024$ (1/ppm 1/mm) in the range $\lambda_{BA} = 288$–313 nm and $\varepsilon_{4F} = 0.0026$ (1/ppm 1/mm) in the range $\lambda_{4F} = 313$–389 nm. The signature of 4F extends until $\lambda \sim 550$ nm. AOT has a signature in the range $\lambda_{AOT} = 232$–262 nm with $\varepsilon = 0.0002$ (1/ppm 1/mm), overlapping with the saturated portion of the asphaltene spectrum. We also measure dispersant solutions in heptane after centrifugation, confirming that the dispersants do not sediment under the given amount of gravitational forcing. To

assess concentrations in the asphaltene suspension supernatants, suspensions are prepared as noted above, and centrifuged for 1000 min at 16 000 *g* (Eppendorf 5415 D). Given ρ_a, this centrifugation time guarantees that asphaltene colloids larger than ~20 nm are driven out of suspension. The resultant supernatants are isolated and measured to assess both the concentration of molecularly dissolved asphaltenes and dispersants.

A summary of the asphaltene and dispersant properties is provided in Table 1. All measurements are carried out at 25 °C and standard pressure.

Results & discussion

Dispersant micellization

To assess the importance of micelles in stabilizing asphaltene colloids we first confirm the critical micelle concentration c_c of the dispersants in heptane alone. Light scattering measurements reveal the presence of micelles once the normalized scattered light intensity I/I_0 increases above its low concentration plateau. At low c in heptane, I/I_0 remains roughly constant for each of the three dispersants, $\sim 5 \times 10^{-6}$. The increase of I/I_0 at c_c indicates a phase transition from isolated dispersant molecules to micelles, at $c = 10$, 100, and 1000 ppm for BA, 4F, and AOT, respectively, in heptane. In contrast, the asphaltene suspensions in heptane scatter two orders of magnitude more light than from the dispersants alone: $I/I_0 \sim 5 \times 10^{-4}$, indicating the presence of colloids. Fig. 1(a) shows I/I_0 for heptane alone (dashed line), the dispersant solutions in heptane (symbols), and the asphaltene suspensions in heptane (solid line). The inset provides a closer look at c_c for each dispersant.

We can compare the c_c of AOT to measured values from the literature, but need a different corroboration of c_c for both BA and 4F. Through various methods of measurements in heptane, including spectrophotometry and calorimetry, the c_c for AOT ranges between 400 and 750 ppm. In octane, decane, and cyclopentane, c_c ranges from 200 to 1100 ppm, whereas in dodecane, the c_c for AOT is ~1250 ppm.[42] Given that AOT is hygroscopic and trace water is difficult to eliminate, the measurement $c_c \sim 1000$ ppm is reasonable when compared to the literature. For BA and 4F, we confirm c_c through conductivity measurements. At low c, the dispersants in heptane have a roughly constant, low conductivity: $\gamma = 0.86 \pm 0.3$ pS. With the formation of micelles, γ increases for both BA and 4F, at values of $c = c_c$ that are in line with the light scattering results. Interestingly, even without dispersants, asphaltene suspensions in heptane have $\gamma = 4.8$ pS, a value reached by the dispersants only at $c \sim 10c_c$. The behavior of γ as a function of BA and 4F

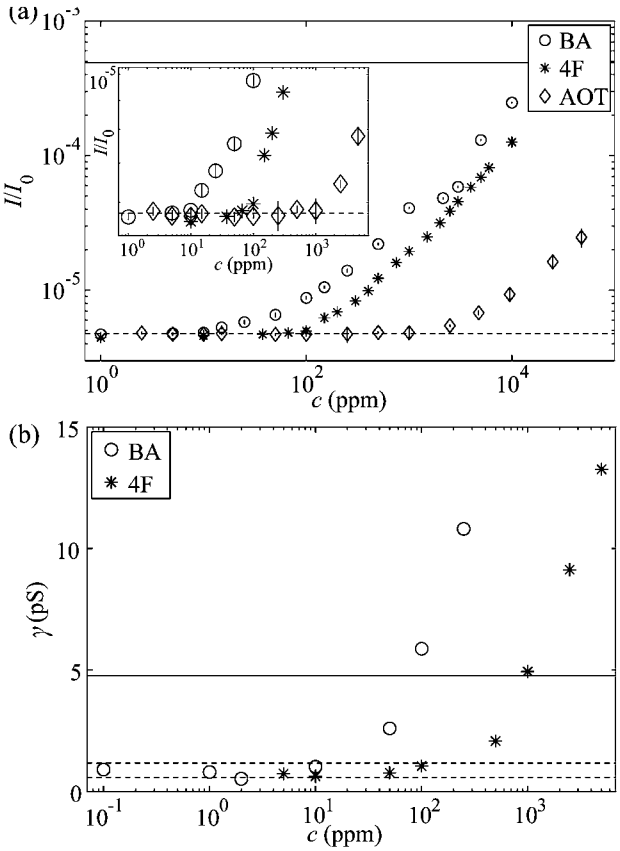

Fig. 1 Evidence of dispersant micellization. (a) shows the normalized intensity of scattered light from dispersant solutions in heptane. The dashed line shows the scattering from heptane alone, while the solid line indicates the amount of scattering with colloidal asphaltenes in suspension. The inset shows the critical micelle concentrations of the dispersants. (b) shows conductivity measurements of dispersant solutions in heptane. The two dashed lines indicate the scatter in the data below c/c_c, while the solid line indicates the conductivity of the asphaltene suspensions in heptane at $c = 0$ ppm.

Table 1 Material properties. Properties extracted from the source petroleum fluid SB: f_c asphaltene fraction in the source fluid, f_a asphaltene fraction in the model oil studied, ρ_a asphaltene density, χ heptane ratio for all suspensions, and ε asphaltene extinction coefficient at $\lambda = 575$ nm. Dispersant information includes dispersant name, class, molecular weight, c_c the critical micelle concentration in heptane, λ the wavelength range used in UV-visible spectroscopy, and ε the dispersant extinction coefficient in the given wavelength range

Petroleum fluid	f_c	f_a	ρ_a (g mL^{-1})	χ (mL g^{-1})	ε (1/ppm 1/mm)
SB	0.0069 ± 0.0008	0.005	1.1 ± 0.09	20	0.0191

Dispersant	Class	MW	c_c (ppm)	λ (nm)	ε (1/ppm 1/mm)
BA	Polyolefin Alkeneamine	2000	10	288–313	0.0024
4F	Alkylated Phenol	4000	100	313–389	0.0026
AOT	Anionic Surfactant	445	1000	232–262	0.0002

concentration in heptane is shown in Fig. 1(b), where the dashed lines indicate the scatter in the low c measurements, and the solid line shows γ for asphaltene suspensions in heptane at $c = 0$ ppm.

Colloidal asphaltene charging

The conductivity of colloidal asphaltene suspensions without dispersant suggests the presence of charge on the asphaltenes themselves. We measure the electrophoretic mobility $\mu = v/E$ of asphaltene colloids suspended in heptane using phase analysis light scattering (PALS), a technique similar to laser Doppler electrophoresis. Particle velocity v in an electric field E is measured by the phase shift in the laser signal compared to a reference signal which does not pass through the electric field. Given the balance of hydrodynamic and electrostatic forces, mobility measurements reflect both the total surface charge q and the particle size a: $\mu \sim q/(6\pi\eta a)$, where η is the viscosity. In suspensions without stabilizing dispersants, the measurements reveal a bimodal distribution of μ: approximately one third of 100 measurements yield negative mobility values, while two thirds yield positive results. The average magnitude of the two modes is roughly equivalent: the average negative mobility is $\langle\mu_-\rangle = (-0.0554 \pm 0.0283) \times 10^{-8}$ m^2 V^{-1} s^{-1}, while $\langle\mu_+\rangle = (0.0561 \pm 0.0261) \times 10^{-8}$ m^2 V^{-1} s^{-1}. For each mode the spread in the distribution $p(\mu)$ is approximately 50%, and may be due in part to a polydispersity in the colloidal asphaltene particle size, to be discussed below. A normalized histogram of the results is shown in Fig. 2; the area under the curve $\int p(\mu)\, d\mu = 1$. The measurements of μ are on the same order of magnitude as the μ of other asphaltenes measured in heptane and heptane-toluene systems.[20,21]

The bimodality of μ suggests that the surfaces of the individual asphaltene colloids may have both positively and negatively charged sites, as depicted in the cartoon in Fig. 2. This situation is more entropically favorable than the possibility of some asphaltene colloids being wholly positively charged while others are wholly negatively charged. The observation of the bimodal distribution of μ is compatible with electrodeposition studies on asphaltenes, which indicate they are charged entities that can exhibit both positive and negative charges.[17–19] Furthermore, conductivity and electrophoresis measurements show evidence of asphaltene ions and ionization even in low dielectric constant media.[7,43] Although the origin of these charges remains somewhat mysterious, asphaltenes are known to contain metallic components whose relative abundance can influence asphaltene dissolution kinetics in heptane with dispersants.[16,44] While metallic components may account for the presence of positive charges, the electron clouds of the π orbitals in the polyaromatic asphaltene rings may provide an explanation for the observed negative charges.

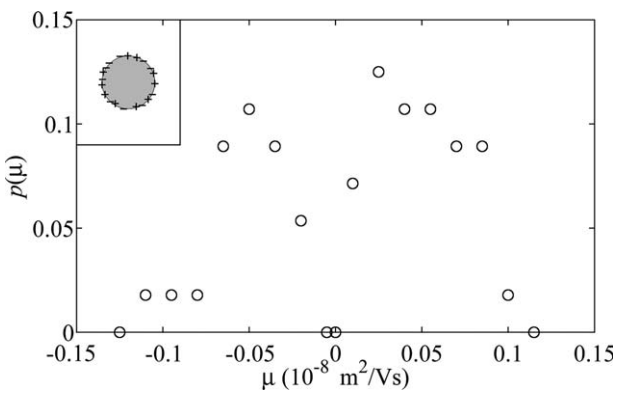

Fig. 2 Distribution of electrophoretic mobility μ in colloidal asphaltene suspensions without dispersant; $p(\mu)$ is based on 100 measurements. The inset gives a representation of charge distribution on an asphaltene colloid.

The observation of mixed charges on the colloidal asphaltene surface indicates a reason for the great instability of colloidal asphaltenes in heptane: no counter-ions exist in the oil to screen the resultant long-range electrostatic attraction, which can readily cause aggregation. Enhanced van der Waals attraction forces have been proposed as the mechanism leading to instability of asphaltenes in non-polar media.[19,45] Van der Waals interactions scale with the ratio of particle size a to interparticle separation r: $U_{vdW} = -A_{121}a/12r$, where A_{121} is the Hamaker constant. Bare coulomb interactions are given by $U_c = -e^2/(4\pi\varepsilon_0 Dr)$, where e is the elementary charge, ε_0 the permittivity of free space and $D = 2$ the dielectric constant of heptane. Both electrostatic and van der Waals interactions decay with the inverse of r, so the range of the two forces is comparable. Given $A_{121} = 1.1 \times 10^{-21}$ for asphaltene-asphaltene interactions in heptane, $U_c = U_{vdW}$ when $a = 1.3$ μm.[46] Therefore, for asphaltene colloids in heptane smaller than ~1.3 μm, electrostatic attraction can be even stronger than van der Waals. In addition to van der Waals, long-range electrostatic attraction due to bimodal surface charging may play an important role in the early stages of asphaltene precipitation and growth approaching the micron scale.

The effect of dispersant on μ is seen when suspensions are prepared by mixing the model oil with stock solutions of dispersants in heptane. We choose two dispersants which have been shown to effectively inhibit aggregation and delay sedimentation in asphaltene suspensions in heptane, labeled 'BA' and '4F'.[8,9] As a point of comparison, we also assess colloidal asphaltene properties with the addition of AOT, known to stabilize non-polar colloidal suspensions through the formation of inverse micelles.[33,38,39] AOT does not provide significant stabilization against aggregation and sedimentation of colloidal asphaltenes in heptane.[8] We refer to all suspensions and results in terms of c/c_c, the normalized dispersant concentration, where c_c is the measured cmc of the dispersants as listed in Table 1.

The addition of even a small amount of the effective dispersants BA and 4F converts the bimodal distribution of μ to a monomodal positive distribution. We quantify this change in $p(\mu)$ through $\int p(\mu_-)\, d\mu$, the total percentage of negative measurements as a function of dispersant. For both BA and 4F, negative charging on the asphaltene colloids persists at low values of c/c_c. In each case the asphaltenes become wholly positively charged at approximately $c/c_c \sim 0.1$. As c/c_c increases, the surface charge remains wholly positive. In contrast, AOT has a nearly opposite effect: below c_c AOT does little to alter $p(\mu)$. Above c_c, AOT micelles facilitate an incomplete negative charging of the asphaltene colloids: ~15% of the measurements remain positive. This result is shown in Fig. 3(a).

We also assess the effect of the dispersants on the average colloidal asphaltene mobilities $\langle\mu\rangle$. Given the bimodal charge distribution $p(\mu)$ without dispersant, $\langle\mu\rangle \sim 0 \times 10^{-8}$ m^2 V^{-1} s^{-1} at $c = 0$ ppm. Both BA and 4F neutralize the negative charges on the asphaltene colloids at $c/c_c = 0.1$, as seen in Fig. 3(a), and additional dispersant continues to increase $\langle\mu\rangle$ even after $\int p(\mu_-)\,d\mu$ reaches 0. Plateau values of $\langle\mu\rangle$ are reached near the c_c of BA and 4F: at $c/c_c \sim 0.7$ for BA and $c/c_c \sim 1.5$ for 4F. In each case the plateaus persist until the highest concentrations measured, $c/c_c = 100$ and 10 for BA and 4F respectively. BA induces a larger magnitude plateau: $\langle\mu\rangle = (0.2296 \pm 0.01) \times 10^{-8}$ m^2 V^{-1} s^{-1}, roughly 24% larger than that induced by 4F: $\langle\mu\rangle = (0.1846 \pm 0.01) \times 10^{-8}$ m^2 V^{-1} s^{-1}. AOT leads to negatively charged asphaltene particles, matching its charge characteristics in other non-polar colloidal suspensions.[39] Contrary to the behavior induced by BA and 4F, the magnitude of $\langle\mu\rangle$ remains flat at $c < c_c$ and changes mainly after the cmc of the AOT is reached. The plateau value is $\langle\mu\rangle = (-0.0638 \pm 0.01) \times 10^{-8}$ m^2 V^{-1} s^{-1}; the error bars encompass the measurement of $\langle\mu_-\rangle$ at $c = 0$. Fig. 3(b) shows $\langle\mu\rangle$ as a function of c/c_c, for suspensions with BA, 4F and AOT. The dashed lines indicate the measured values of $\langle\mu_-\rangle$ and $\langle\mu_+\rangle$ at $c = 0$ ppm. BA and 4F induce plateau values of $\langle\mu\rangle$ that are 3–4 times greater than $\langle\mu_+\rangle$ at $c = 0$ ppm, while AOT does not induce any additional charging beyond $\langle\mu_-\rangle$ at $c = 0$ ppm. With AOT, the plateau in $\langle\mu\rangle$ may reflect simply the negative surface charges already present on the native asphaltenes, suggesting that AOT micelles can neutralize the positive charges which are present on the asphaltenes at $c = 0$ ppm.

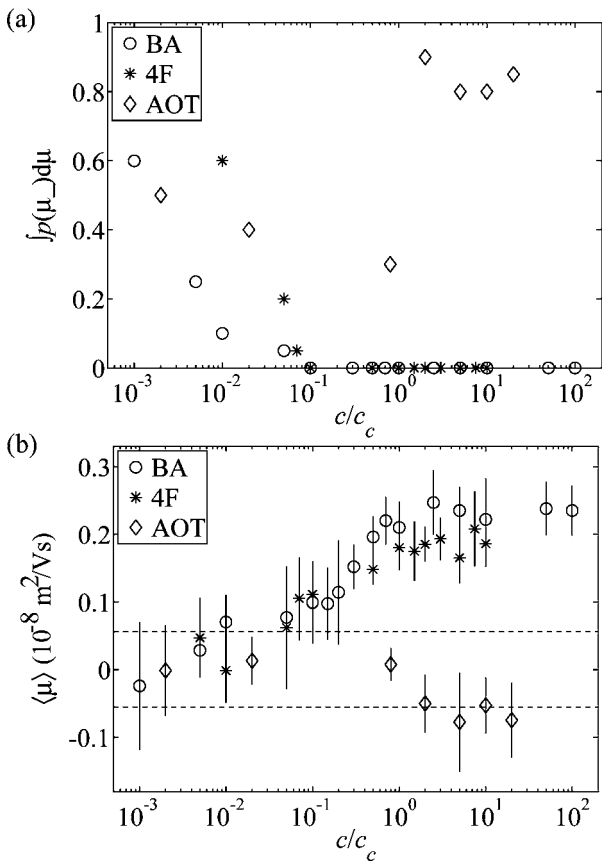

Fig. 3 Electrophoretic mobility of colloidal asphaltenes with dispersant. (a) shows the total percentage of negative mobility measurements as a function of dispersant concentration, while (b) gives $\langle\mu\rangle$ as a function of dispersant concentration. In each plot BA is indicated by (○), 4F by (*) and AOT by (◇). The data in (a) and the error bars in (b) reflect up to 40 measurements at each concentration. The dashed lines in (b) indicate the measurements of $\langle\mu_-\rangle$ and $\langle\mu_+\rangle$ at $c = 0$ ppm.

Dispersant adsorption behavior

The ability of BA and 4F to increase $\langle\mu\rangle$ at $c/c_c < 1$ shows that BA and 4F micelles are not necessary to induce charging; isolated dispersant molecules are sufficient. Below c_c, the dispersant molecules alone do not conduct electricity and are not themselves charge carriers, as evidenced by the measurements shown in Fig. 1(b). However, BA and 4F both contain π bonds through their respective alkene and phenolic functional groups. These π bonds can associate with the aromatic π bonds of asphaltene molecules, potentially explaining the observed coverage of negative surface charges seen in Fig. 3(a). Evidence in the literature suggests that other effective dispersants also act by adsorption.[10,12,47] To discern the dispersant adsorption behavior, we perform UV-visible spectroscopy measurements, first assessing the asphaltene dissolution. We centrifuge the suspensions to remove all asphaltene particles larger than approximately 20 nm, and investigate the suspension supernatants. We use $\lambda = 575$ nm to characterize the amount of molecular-scale asphaltenes in solution, c_{asph}. For all suspensions with BA, 4F and AOT, c_{asph} does not strongly depend on dispersant concentration, and is 61 ± 5 ppm. This amount of molecular-scale asphaltenes is approximately 17% of the total asphaltene content in each suspension, indicating that ~83% of the asphaltene content in each suspension is contained within the colloidal particles.

Having quantified the molecular asphaltenes in the supernatants, we turn our attention to assessing dispersant adsorption. The signature region of AOT overlaps too strongly with the saturated portion of the asphaltene spectra to allow for effective investigation of AOT concentrations. We investigate supernatants prepared using BA and 4F in the wavelength regions λ_{BA} and λ_{4F}, respectively, as listed in Table 1. Asphaltenes also absorb light in these regions: the absorbance $\langle A\rangle$ due to the dissolved asphaltenes is $\langle A\rangle = 1.85 \pm 0.04$ in the region λ_{BA}, while in λ_{4F}, $\langle A\rangle = 1.22 \pm 0.03$. For suspensions with BA, there is little additional absorbance due to dispersant: at all concentrations up to $c/c_c = 100$, $\langle A\rangle \sim 1.86 \pm 0.05$ in the region λ_{BA}. The lack of additional absorbance from BA indicates that the dispersant preferentially adsorbs onto the asphaltenes, remaining with the centrifuged phase. For suspensions with 4F, $\langle A\rangle$ in λ_{4F} remains approximately constant until $c/c_c \sim 2.5$: $\langle A\rangle \sim 1.18 \pm 0.04$, and then rises. However, the observed increase is less than anticipated if all dispersant remained in the supernatant, indicating adsorption onto the asphaltenes in the sedimented phase. The results suggests that BA adsorbs more strongly onto the asphaltenes than 4F, as there is no evidence of BA in the supernatant even up to $c/c_c = 100$. As the behavior of 4F has a stronger trend than that of BA, we show UV-visible spectra of 4F suspension supernatants in Fig. 4, where the solid line shows the spectrum due to the dissolved asphaltenes alone. The inset gives $\langle A\rangle$ as a function of c/c_c in the range λ_{4F} as compared to both $\langle A\rangle$ for the dissolved asphaltenes (solid horizontal line) and

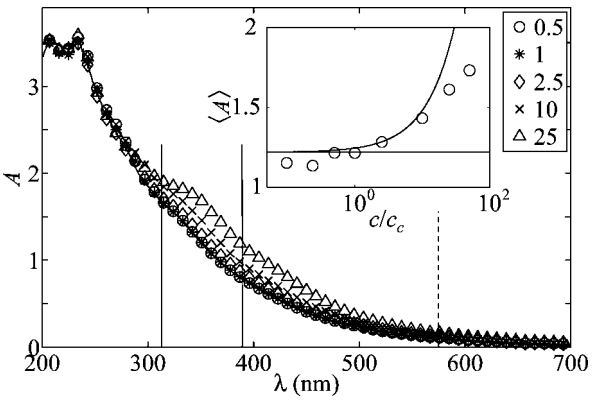

Fig. 4 UV-visible spectroscopy on asphaltene suspension supernatants. The main plot shows several spectra of supernatants with 4F, at c/c_c as given in the legend. The spectrum shown by the solid line shows the behavior at $c/c_c = 0$. The dashed line indicates $\lambda = 575$ nm used to characterize the asphaltene content, while the pair of solid lines denotes the range $\lambda_{4F} = 313$–389 nm. The inset shows $\langle A \rangle$ as function of c/c_c in this range; the solid line indicates $\langle A \rangle$ due to the dissolved asphaltenes, while the curve indicates $\langle A \rangle$ due to the dispersant.

the expected increase from equivalent amounts of 4F in the supernatant (solid curve).

Asphaltene particle size and morphology

The adsorption of BA and 4F onto the asphaltene surface may affect asphaltene particle size and morphology. Optical microscopy studies show that asphaltenes in heptane form round, compact structures.[48] Furthermore, a decrease in colloidal asphaltene size with the addition of dispersant has been previously observed, but without explanation.[8,9,49] We first investigate the colloidal asphaltene suspensions in the absence of dispersant, using dynamic light scattering (DLS) to measure the colloidal asphaltene particle size a. Within the first minute, the time between sample preparation and the start of the measurement, the asphaltenes have already grown from the molecular scale to $a \sim 1$ μm, and continue to grow over the next 10–15 min. The growth leads to a plateau $\langle a \rangle = 3.13 \pm 0.46$ μm, with the 20% variation indicating a high degree of polydispersity. The early-time growth of the asphaltene colloids without dispersant is shown in Fig. 5(a).

With the addition of a small amount of BA or 4F, the colloids do not grow to the same final size, and $\langle a \rangle$ decreases dramatically, beginning at $c/c_c = 0.01$ in the BA suspensions and $c/c_c = 0.02$ with 4F. The size decreases until $c/c_c \sim 0.5$, followed by a plateau at $\langle a \rangle = 204 \pm 21$ nm. BA and 4F cause a 15-fold decrease in $\langle a \rangle$ at $c/c_c = 1$ as compared to $c/c_c = 0$. Furthermore, once $\langle a \rangle$ decreases into the nanometre range, the distribution width in the suspensions also decreases, to $\sigma/a < 4\%$, indicating fairly monodisperse suspensions with the addition of BA and 4F. AOT, however, does not halt the colloidal asphaltene growth nor significantly alter $\langle a \rangle$ as compared to the value at $c/c_c = 0$, even at concentrations ten times larger than c_c. The average particle size over all suspensions with AOT is 2.98 μm, and the distribution width in each sample is $\sigma/\langle a \rangle \sim 17\%$, indicating fairly polydisperse suspensions regardless of AOT concentration. The

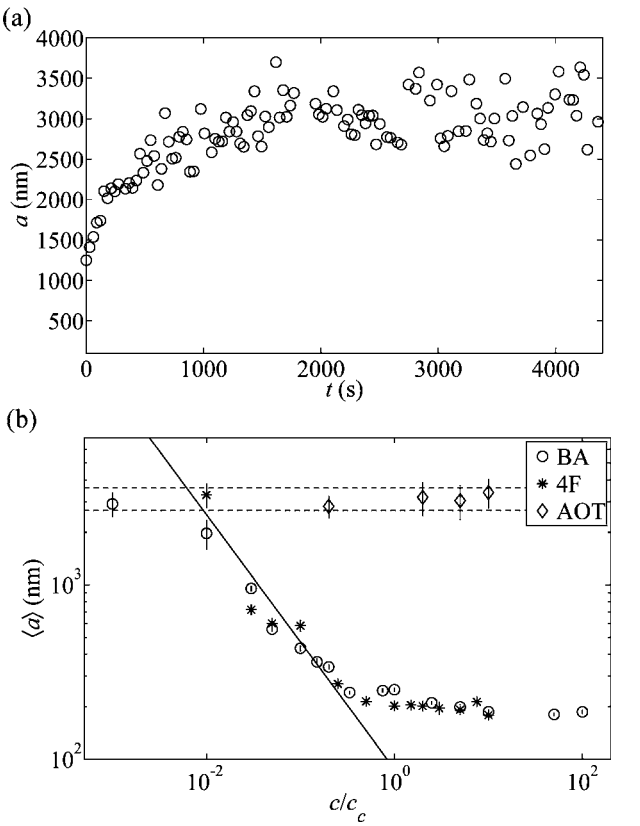

Fig. 5 Colloidal asphaltene particle sizes. (a) shows the growth of the asphaltene colloids without dispersant, followed by a plateau at size $\langle a \rangle$. (b) shows $\langle a \rangle$ as a function of dispersant concentration, with BA (○), 4F (*) and AOT (◇), displayed on a log-log plot. The error bars in (b) show the size distribution σ of ~120 measurements at each c/c_c. The dashed lines indicate σ at $c = 0$. The solid black line is a fit to the data, with slope −0.73.

behavior of $\langle a \rangle$ with all three dispersants is shown in Fig. 5(b), on a log scale to better illustrate the decrease at $c < c_c$ and the plateau at $c > c_c$ for suspensions with BA and 4F. The error bars indicate σ in each sample and the dashed lines indicate σ in suspensions without dispersant. The solid line indicates a power-law fit to $\langle a \rangle$ at concentrations $0.01 < c/c_c < 0.5$.

The power-law decrease in $\langle a \rangle$ with BA and 4F may be explained by a simple scaling argument describing the effect of dispersant adsorption on $\langle a \rangle$. These measurements show that dispersants BA and 4F truncate the initial stages of colloidal asphaltene growth. If the molecules of dispersant uniformly adsorb onto the asphaltene particle surfaces, then for suspensions with constant asphaltene mass we expect the surface area to volume ratio S_V to increase linearly with c, allowing for smaller particles. For fractal objects, $S_V \sim \langle a \rangle^{(D_f-3)}$, where D_f is the fractal dimension.[50] Simple scaling therefore gives a power law dependence of $\langle a \rangle$ on c: $\langle a \rangle^{(D_f-3)} \sim c$, with the expected decrease in $\langle a \rangle$ with the addition of dispersant.

To test the validity of the scaling argument in comparison to the observed power law behavior of $\langle a \rangle$ with BA and 4F, we characterize the fractal structure of the asphaltene colloids. We employ static light scattering (SLS), a standard method by which to measure the fractal dimension D_f, as the scattered light

intensity scales as $I = q^{-D_f}$, where q is the wave vector.[50] We investigate a dozen suspensions with BA and 4F over a range of c/c_c and find that D_f has a slight dependence on c/c_c, decreasing from ~1.8 at $c/c_c = 0$ to ~ 1.5 at $c/c_c = 1$. The average value D_f is 1.63 ± 0.16, a variation of 10%. Representative results are shown in Fig. 6, as shown by suspensions at $c = 0$ and at $c < c_c$ for BA and 4F. The solid black lines indicate fits to the data. The value $D_f = 1.63$ suggests the power law $\langle a \rangle \sim c^{-0.73}$, which fits the measurements of $\langle a \rangle$ with an R^2 value of 0.96, as shown by the solid line in Fig. 5(b).

The present results indicate a unique stabilization mechanism found in non-polar colloidal asphaltene suspensions: the adsorption of single molecules of surfactant simultaneously provides electrostatic stabilization and truncates colloidal growth. The dual-charge nature of the asphaltenes at $c/c_c = 0$ explains their affinity for growth. At $c \leq c_c$ of effective dispersants BA and 4F: the dispersants adsorb, the asphaltene colloids become uniformly charged and $\langle \mu \rangle$ increases up to $c = c_c$. The uniformly positive surface charge truncates further growth of the asphaltenes, which grow to increasingly smaller sizes, with a power-law dependence on c/c_c. We therefore propose that single dispersant molecules stabilize asphaltenes by coating colloidal asphaltenes, in this case preferentially covering negatively charged sites on the surface. In fact, the increase in $\langle \mu \rangle$ with the addition of dispersant can be qualitatively explained by the corresponding decrease in $\langle a \rangle$. Cartoons of this mechanism are provided in Fig. 7. We note that this mechanism may not otherwise work in traditional colloidal systems: the bimodal charge on the asphaltene colloids at $c/c_c = 0$ plays a key role in allowing both the dispersant adsorption and subsequent suspension stabilization to occur.

Conclusions

Contrary to the current understanding of electrostatic stabilization of non-polar colloids, inverse micelles of dispersant at $c > c_c$ are not necessary to induce charge-stabilization in non-polar suspensions of asphaltene colloids. Isolated dispersant molecules adsorb onto asphaltene colloids as they grow, neutralize the negative surface charges, induce uniformly positive surfaces, and thereby truncate colloidal growth. The appearance of micelles of BA and 4F at the cmc can explain both the ceiling in $\langle \mu \rangle$ and the floor in $\langle a \rangle$. Exceeding the cmc limits the number of isolated dispersant molecules and halts the stabilization process rather than providing further changes in the colloidal asphaltene properties. AOT provides an excellent counter-example: while measurements of $\langle \mu \rangle$ indicate that AOT micelles can neutralize most of the positive surface charges on the asphaltene colloids, the absence of any effect on $\langle a \rangle$ indicates that AOT does not effectively truncate colloidal asphaltene growth even above c_c. The dichotomy between AOT and BA or 4F raises an interesting possibility for future investigation: adsorption onto positive asphaltene surface charges might not effectively truncate growth, while adsorption onto negative surface charges can, as it is the π bonds which are the main drivers of asphaltene instability.[44] Furthermore, our work introduces the cmc as an important consideration in industrial dispersant selection. Both the polarity or acidity of the headgroups as well as the length and branching of the tails have been shown to be important characteristics of dispersants.[10,11,13–15] Until now considerations of the cmc have been largely ignored. While a low cmc does not guarantee effectiveness, the fact that c_c for BA is less than that for 4F means that 10 times less BA is needed to obtain similar results.

The observed bimodal charge distribution on asphaltenes in non-polar suspensions facilitates their growth and aggregation to the colloidal scale and beyond. Selective adsorption of effective dispersants to the colloidal asphaltene surface can truncate this growth, offering the ability to tune colloidal asphaltene properties in non-polar suspensions, including final size and

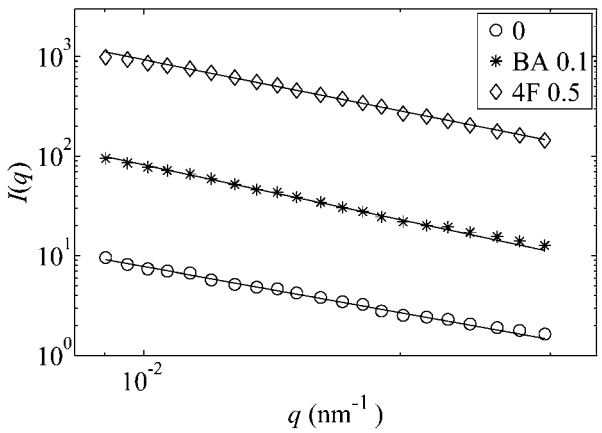

Fig. 6 Fractal dimension measurements. Static light scattered intensity from asphaltene suspensions without dispersant, with BA at $c/c_c = 0.1$ and with 4F at $c/c_c = 0.5$. The solid lines are fits to the data; the slopes provide D_f. $I(q)$ for each sample has been multiplied by an arbitrary constant for better visualization of the data.

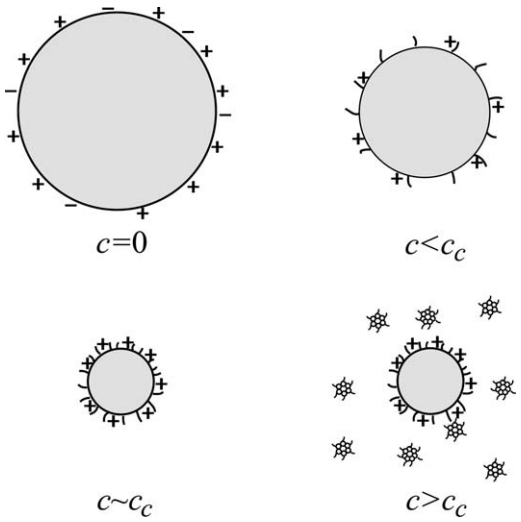

Fig. 7 Proposed stabilization mechanism. At $c = 0$, the asphaltene colloids display both positive and negative surface charges. At low dispersant concentration, $c < c_c$, isolated dispersant molecules adsorb onto the colloidal surface, neutralizing negative charges. Increasing surface coverage truncates the asphaltene particle growth until the dispersant cmc is reached. At $c > c_c$, dispersant micelles might adsorb onto the surface, but their presence effects neither the size nor the mobility of the colloids. The figure is not drawn to scale.

electrophoretic mobility. There is even some indication that the asphaltene colloids become more compact as they grow to larger sizes, as evidenced by the slightly higher values of D_f found at low concentration of dispersant. Given their unique charge characteristics, asphaltenes may therefore provide an interesting platform for further investigation of remaining open questions about electrostatic stabilization in non-polar media.[51] The development and synthesis of model asphaltene particles could even result in novel functional materials. For instance, many applications of photonic materials, including switchable electrophoretic displays used for electronic ink, rely on sub-micron colloidal size scales and the tunable response of particles to external fields.[52,53]

Acknowledgements

We gratefully acknowledge the support of RERI member institutions. SMH thanks Eric Dufresne, Ian Morrison and Chinedum Osuji for helpful conversations, and Menachem Elimelech for the use of his ALV light scattering equipment.

References

1 O. C. Mullins, *Energy Fuels*, 2010, **24**, 2179–2207.
2 Z. Li and A. Firoozabadi, *Energy Fuels*, 2010, **24**, 1106–1113.
3 Z. Li and A. Firoozabadi, *Energy Fuels*, 2010, **24**, 2956–2963.
4 M. A. Anisimov, I. K. Yudin, V. Nikitin, G. Nikolaenko, A. Chernoutsan, H. Toulhoat, D. Frot and Y. Briolant, *J. Phys. Chem.*, 1995, **99**, 9576–9580.
5 Y. G. Burya, I. K. Yudin, V. A. Dechabo, V. I. Kosov and M. A. Anisimov, *Appl. Opt.*, 2001, **40**, 4028.
6 T. G. Mason and M. Y. Lin, *Phys. Rev. E: Stat. Phys., Plasmas, Fluids, Relat. Interdiscip. Top.*, 2003, **67**, 050401.
7 B. Siffert, J. Kuczinski and E. Papirer, *J. Colloid Interface Sci.*, 1990, **135**, 107.
8 S. M. Hashmi, L. A. Quintiliano and A. Firoozabadi, *Langmuir*, 2010, **26**, 8021.
9 S. M. Hashmi and A. Firoozabadi, *J. Phys. Chem. B*, 2010, **114**, 15780–15788.
10 C.-L. Chang and H. S. Fogler, *Langmuir*, 1994, **10**, 1749–1757.
11 P. Permsukarome, C. Chang and H. S. Fogler, *Ind. Eng. Chem. Res.*, 1997, **36**, 3960–3967.
12 O. León, E. Contreras, E. Rogel, G. Dambakli, J. Espidel and S. Acevedo, *Energy Fuels*, 2001, **15**, 1028–1032.
13 T. A. Al-Sahhaf, M. A. Fahim and A. S. Elkilani, *Fluid Phase Equilib.*, 2002, **194–197**, 1045–1057.
14 I. A. Wiehe and T. G. Jermansen, *J. Pet. Sci. Eng.*, 2003, **21**, 527–536.
15 L. C. Rocha Junior, M. S. Ferreira and A. Carlos da Silva Ramos, *J. Pet. Sci. Eng.*, 2006, **51**, 26–36.
16 T. J. Kaminski, H. S. Fogler, N. Wolf, P. Wattana and A. Mairal, *Energy Fuels*, 2000, **14**, 25–30.
17 G. W. Preckshot, N. G. Delisle, C. E. Cottrell and D. L. Katz, *AIME Trans.*, 1943, **151**, 188–194.
18 D. L. Katz and K. E. Beu, *Ind. Eng. Chem.*, 1945, **43**, 1165.
19 S. E. Taylor, *Fuel*, 1998, **77**, 821–828.
20 O. León, E. Rogel, G. Torres and A. Lucas, *Pet. Sci. Technol.*, 2000, **18**, 913–927.
21 G. Gonzalez, G. B. M. Neves, S. M. Saraiva, E. F. Lucas and M. dos Anjos de Sousa, *Energy Fuels*, 2003, **17**, 879–886.
22 H. Parra-Barraza, D. Hernandez-Montiel, J. Lizardi, J. Hernandez, R. H. Urbina and M. A. Valdez, *Fuel*, 2003, **82**, 869–874.
23 I. K. Yudin and M. A. Anisimov, in *Asphaltenes, Heavy Oils and Petroleomics*, ed. O. C. Mullins, E. Y. Sheu, A. Hammami and A. G. Marshall, Springer New York, New York, 2007, pp. 439–468.
24 T. A. Witten and P. A. Pincus, *Macromolecules*, 1986, **19**, 2509–2513.
25 E. B. Zhulina, O. V. Borisov and V. A. Priamitsyn, *J. Colloid Interface Sci.*, 1990, **137**, 495–511.
26 P. F. Luckham, *Adv. Colloid Interface Sci.*, 1991, **34**, 191–215.
27 R. J. Pugh, T. Matsunaga and F. M. Fowkes, *Colloids Surf.*, 1983, **7**, 183.
28 L. Antl, J. W. Goodwin, R. D. Hill, R. H. Ottewill, S. M. Owens, S. Papworth and J. A. Waters, *Colloids Surf.*, 1986, **17**, 67.
29 S. M. Underwood, J. R. Taylor and W. van Megen, *Langmuir*, 1994, **10**, 3550–3554.
30 S. E. Phan, W. B. Russel, J. Zhu and P. M. Chaikin, *J. Chem. Phys.*, 1998, **108**, 9789–9795.
31 Y.-Y. Won, S. Meeker, V. Trapp, D. A. Weitz, N. Z. Diggs and J. I. Emert, *Langmuir*, 2005, **21**, 924–932.
32 S. Auer, W. C. K. Poon and D. Frenkel, *Phys. Rev. E: Stat. Phys., Plasmas, Fluids, Relat. Interdiscip. Top.*, 2003, **67**, 020401.
33 S. K. Sainis, V. Germain, C. O. Mejean and E. R. Dufresne, *Langmuir*, 2008, **24**, 1160–1164.
34 J. L. van der Minne and P. H. J. Hermanie, *J. Colloid Sci.*, 1953, **8**, 38.
35 F. M. Fowkes, in *Solvent Properties of Surfactant Solutions*, ed. K. Shioda, Marcel Dekker, New York, 1967, pp. 65–115.
36 R. J. Pugh, T. Matsunaga and F. M. Fowkes, *Colloids Surf.*, 1983, **7**, 183–207.
37 I. D. Morrison, *Colloids Surf., A*, 1993, **71**, 1.
38 K. Osseo-Asare and F. J. Arriagada, *Colloids Surf.*, 1990, **50**, 321–339.
39 M. F. Hsu, E. R. Dufresne and D. A. Weitz, *Langmuir*, 2005, **21**, 4881–4887.
40 S. Poovarodom and J. C. Berg, *J. Colloid Interface Sci.*, 2010, **346**, 370–377.
41 G. S. Roberts, R. Sanchez, R. Kemp, T. Wood and P. Bartlett, *Langmuir*, 2008, **24**, 6530.
42 C.-C. Huang and K. L. Hohn, *J. Phys. Chem. B*, 2010, **114**, 2685–2694.
43 P. Fotland and H. Anfindsen, *Fuel Sci. Technol. Int.*, 1996, **14**, 109–125.
44 H. Groenzin and O. C. Mullins, *Energy Fuels*, 2000, **14**, 677–684.
45 J. R. Wright and R. R. Minesinger, *J. Colloid Sci.*, 1963, **18**, 223–236.
46 S. Wang, J. Liu, L. Zhang, J. Masliyah and Z. Xu, *Langmuir*, 2010, **26**, 183–190.
47 M. Barcenas, P. Orea, E. Buenrostro-González, L. S. Zamudio-Rivera and Y. Duda, *Energy Fuels*, 2008, **22**, 1917–1922.
48 E. S. Boek, H. K. Ladva, J. P. Crawshaw and J. T. Padding, *Energy Fuels*, 2008, **22**, 805–813.
49 F. Arteaga-Larios, A. Cosultchi and E. Perez, *Energy Fuels*, 2005, **19**, 477–484.
50 P. C. Hiemenz and R. Rajagopalan, *Principles of Colloid and Surface Chemistry*, Marcel Dekker, Inc., New York, NY, 1997.
51 J. W. Merrill, S. K. Sainis and E. R. Dufresne, *Phys. Rev. Lett.*, 2009, **103**, 138301.
52 B. Comiskey, J. D. Albert, H. Yoshizawa and J. Jacobson, *Nature*, 1998, **394**, 253–255.
53 Y. Chen, J. Au, P. Kazlas, A. Ritenour, H. Gates and M. McCreary, *Nature*, 2003, **423**, 136–137.